Probing the Roughness of Porphyrin Thin Films with X-ray Photoelectron Spectroscopy

Elmar Kataev,*[a] Daniel Wechsler,[a] Federico J. Williams,[b] Julia Köbl,[a] Natalia Tsud,[c] Stefano Franchi,[d] Hans-Peter Steinrück,[a] and Ole Lytken[a]

Thin-film growth of molecular systems is of interest for many applications, such as for instance organic electronics. In this study, we demonstrate how X-ray photoelectron spectroscopy (XPS) can be used to study the growth behavior of such molecular systems. In XPS, coverages are often calculated assuming a uniform thickness across a surface. This results in an error for rough films, and the magnitude of this error depends on the kinetic energy of the photoelectrons analyzed. We have used this kinetic-energy dependency to estimate the roughnesses of thin porphyrin films grown on rutile TiO_2(110). We used two different molecules: cobalt (II) monocarboxyphenyl-10,15,20-triphenylporphyrin (CoMCTPP), with carboxylic-acid anchor groups, and cobalt (II) tetraphenylporphyrin (CoTPP), without anchor groups. We find CoMCTPP to grow as rough films at room temperature across the studied coverage range, whereas for CoTPP the first two layers remain smooth and even; depositing additional CoTPP results in rough films. Although, XPS is not a common technique for measuring roughness, it is fast and provides information of both roughness and thickness in one measurement.

1. Introduction

Understanding the growth of organic thin films is crucial for the new optoelectronic era, with its organic thin film transistors,[1] photovoltaics[2] and light emitting diodes.[3] The growth and thereby structure of the films is important because it affects critical parameters such as electronic structure and charge transport..[1e,4] Growth and structure are complicated phenomena and depend strongly on the surface used as template for the growth. Films can be crystalline or disordered.[5] Structural transitions are also possible, sometimes after the first layer, sometimes even during the growth of the multilayer.[5a,6] Thermal annealing may also affect the films and lead to a reorganization of the molecules,[5a,7] sometimes accompanied by partial desorption.

We will focus on the thin film growth and temperature-dependent behavior of two different porphyrin molecules on rutile TiO_2(110). Porphyrins consist of four pyrrole rings linked by methine groups, creating a central cavity surrounded by four nitrogen atoms, see Figure 1. This central cavity can coordinate either two protons, creating a free-base porphyrin, or it can coordinate a metal center, creating a metalloporphyrin. Depending on the central metal atom and potential side groups, porphyrins exist with a wide range of chemical, biological, and electronic functionalities.[8] Owing to their structural flexibility, they find widespread applications in electrocatalysis,[9] sensorics,[10] molecular electronics,[11] molecular mechanics[12] and dye-sensitized solar cells.[13] To be used in devices, the molecules have to be supported on solid substrates. Because of this, the adsorption of porphyrins on metal and to some extent oxide surfaces have been studied extensively.[6c,8,14] However, most studies only focus on the first layer, and far fewer studies exist where the coverage has been extended into the multilayers.[15] Because the structure of the first layer is critical for the growth, we have chosen two different porphyrin

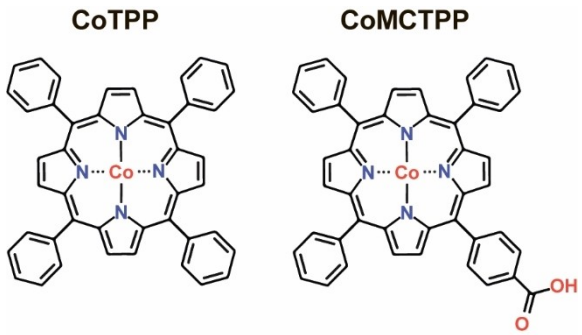

Figure 1. Structures of cobalt (II) 5,10,15,20-tetraphenylporphyrin (CoTPP) and cobalt(II) 5-monocarboxyphenyl-10,15,20-triphenylporphyrin (CoMCTPP).

[a] *Dr. E. Kataev, D. Wechsler, J. Köbl, Prof. H.-P. Steinrück, Dr. O. Lytken*
Department of Chemistry and Pharmacy
Friedrich-Alexander Universität Erlangen-Nürnberg
Egerlandstraße 3, Erlangen, 91058, Germany
E-mail: elmar.kataev@fau.de
[b] *Prof. F. J. Williams*
Departamento de Química Inorgánica, Analítica y Química Física
Universidad de Buenos Aires
Pabellón 2, Buenos Aires C1428EHA, Argentina
[c] *Dr. N. Tsud*
Department of Surface and Plasma Science
Charles University
V Holešovičkách 2, Prague, 11636, Czech Republic
[d] *Dr. S. Franchi*
Istituto di Struttura della Materia
Consiglio Nazionale delle Ricerche
via Fosso del Cavaliere, 100, Roma, Italy

molecules: one with and one without a carboxylic-acid anchoring group. This should strongly affect the structure of the first layer. The two molecules are cobalt(II) 5-monocarboxyphenyl-10,15,20-triphenylporphyrin (CoMCTPP) and cobalt(II) tetraphenylporphyrin (CoTPP), see Figure 1. Based on previous studies, we expect CoTPP, without the carboxylic-acid anchor group, to adsorb flat-flying in the first layer,[16] whereas the anchoring groups of CoMCTPP should cause it to adsorb with a more upright-standing orientation.[6c,14i]

Atomic force microscopy (AFM) is the universal tool for probing surface morphology of organic thin films.[4b,6a,17] Beautiful examples of complex growth behaviors studied by AFM include fractal structures,[6a,17c] needles[18] and dendrites.[4b,17a,e] However, AFM is not able to measure the thicknesses of the deposited films.[19] To obtain this information, AFM has to be combined with supplemental techniques, such as X-ray photoelectron spectroscopy (XPS). The thickness characterization is especially crucial for elevated temperatures where desorption of molecules may occur.

We will demonstrate how kinetic-energy-dependent synchrotron-radiation XPS can be used to measure not only thicknesses but also roughnesses of thin films. This approach will never achieve the same detailed topological information provided by AFM, but it is an interesting alternative for situations where only a single descriptor of the surface, such as roughness, is desired. Synchrotron-radiation XPS is also fast, and therefore useful for exploring large parameter spaces, such as temperature and coverage. Kinetic-energy-dependent XPS has previously been used to distinguish between layer-by-layer and 3D growth,[20] but to the best of our knowledge XPS has not previously been used to quantify roughnesses of thin films.

2. Methodological Background

XPS is one of the most-used methods in surface science. From the days of Siegbahn,[21] XPS has provided both qualitative information about elements present in the near-surface region and their oxidation states as well as quantitative information about the thicknesses of thin films or concentration of elements. The thicknesses of thin films are what we are interested in.

We will start with some basic information on quantitative XPS: Any film deposited on a substrate will attenuate the photoelectrons emitted from the substrate. For thin even films, this attenuation follows a simple exponential decay law, which for porphyrin thin films on TiO_2(110) can be written as:

$$I_{Ti} = I^0_{Ti} \cdot \exp(-h/\lambda_{Ti}) \quad (1)$$

where I_{Ti} is the attenuated Ti 3p signal from the TiO_2 substrate, I^0_{Ti} is the Ti 3p signal from a clean substrate, h is the thickness of the film and λ_{Ti} is the inelastic mean free path of the Ti 3p photoelectrons travelling through the porphyrin film. The Ti 3p core level was used instead of Ti 2p, because it allowed us to measure a wider kinetic energy range. The C 1s signal from the porphyrin thin film can be described in a similar fashion:

$$I_C = I^0_C \cdot (1 - \exp(-h/\lambda_c)) \quad (2)$$

where I_C is the C 1s signal from the porphyrin film, I^0_C is the signal from an infinitely thick film, h is the thickness of the film, and λ_c is the inelastic mean free path of the C 1s photoelectrons travelling through the porphyrin film. Either the Ti 3p or the C 1s signal can in principle be used to calculate the thickness of the film, but the best accuracy is achieved when the ratio of the two signals is used. If the photon energies are chosen to give the same kinetic energy for both core levels, the photoelectrons will have the same inelastic mean free path ($\lambda = \lambda_C = \lambda_{Ti}$), and we can combine the equations for the intensities of the Ti 3p and C 1s signals into a single equation:

$$I_{C/Ti} = I^0_{C/Ti} \cdot (\exp(h/\lambda) - 1) \quad (3)$$

where $I_{C/Ti}$ is the ratio of the C 1s and Ti 3p signals, $I^0_{C/Ti}$is the ratio of the C 1s signal from an infinitely thick porphyrin film and the Ti 3p signal from a clean TiO_2 surface, h is the thickness of the film, and λ is the inelastic mean free path of the C 1s and Ti 3p photoelectrons. This equation can now easily be rearranged to calculate the thickness of the film:

$$h = \lambda \cdot \ln\left(I_{C/Ti}/I^0_{C/Ti} + 1\right) \quad (4)$$

or to calculate the inelastic mean free path of the photoelectrons, if the thickness of the film is already known:

$$\lambda = h/\ln\left(I_{C/Ti}/I^0_{C/Ti} + 1\right) \quad (5)$$

An alternative and more appropriate name for λ would be "effective escape depth", since elastic scattering also contributes to the attenuation, but the term "inelastic mean free path" is typically used.

The above equations describe how film thicknesses are calculated in XPS (for a nice introduction into XPS we recommend additional literature[22]). However, they are only true for even films with no thickness variations. If the films are not even, the "apparent" thicknesses calculated from XPS will be smaller than the true thicknesses of the films. The magnitude of the difference depends on the length of the inelastic mean free path compared to the thickness of the film. If the inelastic mean free path is long and the substrate signal barely attenuated, thickness variations will only have small effects on the measured apparent thicknesses. However, if the inelastic mean free path is short and the attenuation of the substrate signal significant, a variation in thickness will have a large effect and the measured apparent thickness will significantly underestimate the real average thickness of the film.

Several approaches have been suggested to reduce the error in the measured thicknesses,[23] however we are going to use them to quantify the roughnesses of porphyrin thin films on TiO_2(110). Simply put, we will use the above equations to calculate the apparent thicknesses of several porphyrin thin

films, but we will do so using four different kinetic energies and thereby four different inelastic mean free paths of the photoelectrons. If the four calculations agree with each other, the film is evenly thick. If the four calculations deviate from each other, the film is not even, and the magnitude of the difference is correlated with the roughness of the film. Further down, we will convert these discrepancies into roughnesses in monolayers, but for now we will focus on the qualitative picture. It is worth mentioning that very similar measurements are possible with laboratory X-ray sources by varying the emission angle.[23a,24] However, shadowing and elastic scattering complicates the analysis at grazing emission.[23a,25] Another possibility would be to follow several photoemission lines with different binding energies, resulting in different kinetic energies of the emitted photoelectrons.[26]

3. Results and Discussion

We chose two different molecules to investigate on rutile TiO_2(110): CoTPP, without a covalent anchor group, and CoMCTPP, which has a carboxylic-acid anchor group, see Figure 1. From literature we know that CoTPP adsorbs in a flat-lying geometry in the first layer,[16] whereas CoMCTPP adsorbs in a tilted geometry.[14i] This results in very different interactions between the first and second layers for the two molecules and should have a significant impact on their growth behavior.

Before we can use Equation 4 to calculate film thicknesses a few reference measurements are needed. For each kinetic energy, we measured the Ti 3p intensity of a clean TiO_2 surface (I^0_{Ti}) as well as the C 1s intensity from a sufficiently thick layer of porphyrin molecules such that the Ti 3p signal has completely vanished (I^0_C). Lastly, we used the annealed CoMCTPP monolayer left on the surface after annealing to 480 K and above as a reference for a thin even film with a coverage we define to be one monolayer.

Specifically, we created coverage gradients from one to six monolayers across our TiO_2(110) single-crystal surface. We then measured C 1s and Ti 3p synchrotron-radiation photoemission spectra for four different kinetic energies: 100, 200, 400 and 700 eV, while heating stepwise to 500 K (10 K per step). Selected raw photoemission spectra are displayed in Figure 2, while the apparent thicknesses calculated using Equation 4 as a function of coverage and temperature are presented in Figure 3. Looking at Figure 3, it is readily clear that the two molecules behave very differently. For CoTPP, we observe no kinetic-energy dependence at low coverage, indicating an even film and layer-by-layer growth mode. For CoMCTPP, we observe significant discrepancies between the kinetic energies at all coverages, with lower kinetic energies resulting in lower apparent coverages, as expected for uneven films. However, for both molecules we observe no rearrangement within the films upon heating: the roughness is constant until the multilayer desorbs.

Keen observers among the readers will have noticed that the thickness of the annealed CoTPP monolayer in Figure 3, remaining after multilayer desorption at 420 K, is only 0.5 ML

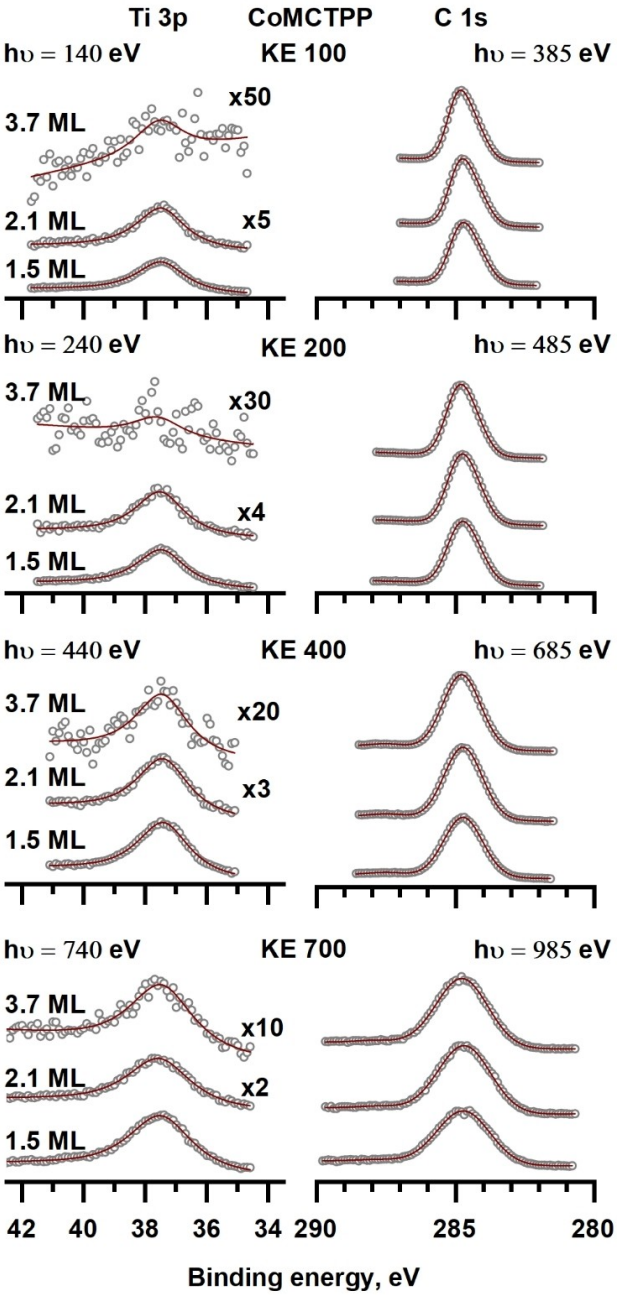

Figure 2. Selected raw photoemission spectra for high, medium and low coverages of CoMCTPP. In total, more than 3000 spectra were measured. The coverages indicated are the apparent thicknesses calculated with Equation 4 for a kinetic energy of 700 eV and correspond to the apparent thicknesses in Figure 3. To minimize the uncertainty of the fitted peak areas, no peak parameters other than area and Shirley background were allowed to change with coverage. To ensure maximum intensity, the widest possible monochromator slits were used, producing very broad peaks and thus widening of the peaks is not related to changes of the chemical state.

thick. However, keep in mind that we defined one monolayer as the number of molecules equivalent to the annealed CoMCTPP monolayer. A thickness of X monolayers should therefore not be understood as X physical layers, but rather as X times the number of molecules in the tilted CoMCTPP monolayer. It now becomes clear that the CoTPP monolayer, therefore, must

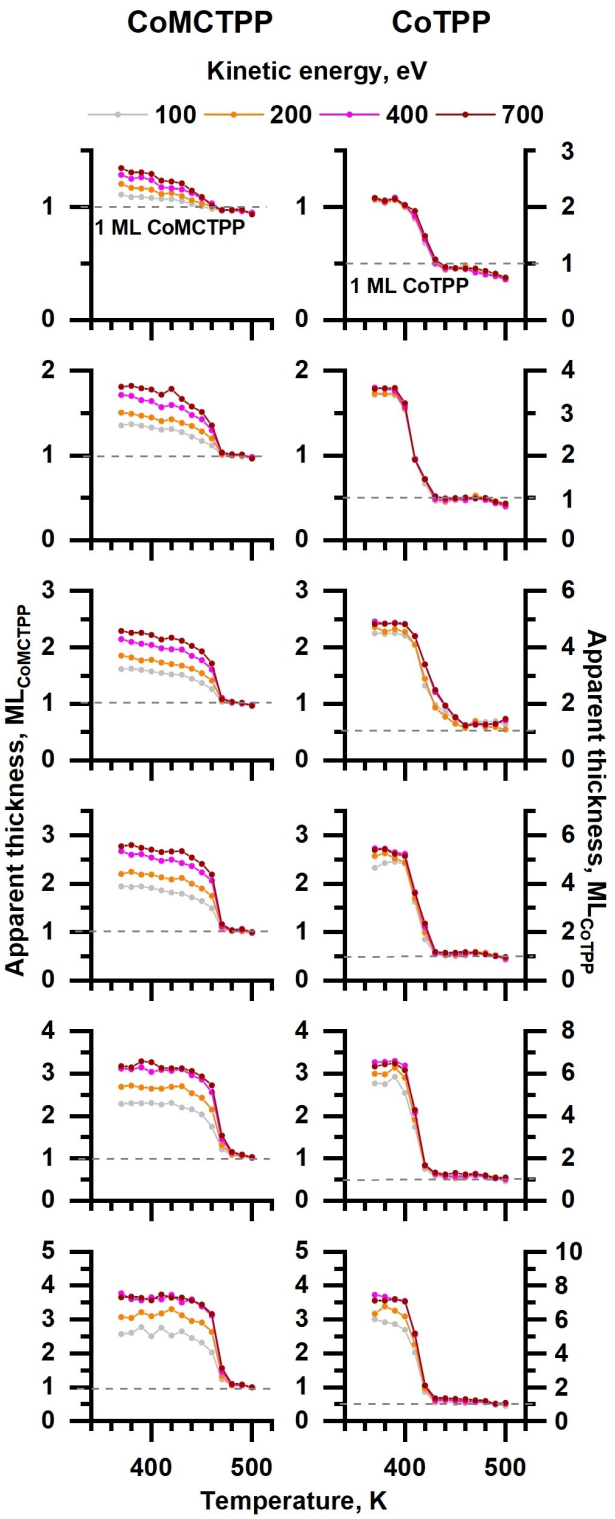

Figure 3. Apparent film thicknesses for CoTPP and CoMCTPP, calculated using Equation 4, as a function of increasing coverage (top to bottom), temperature and kinetic energy. The left axis is in units of CoMCTPP monolayers and the right in units of CoTPP monolayers (see text for details).

contain half the number of molecules of the CoMCTPP monolayer, consistent with the tilted monolayer of CoMCTPP being more densely packed than the flat-lying layer of CoTPP.[14i] For convenience, we have included an additional coverage axis in units of CoTPP monolayers on the right side of most figures.

In order to calculate the apparent coverages in Figure 3 we need the mean free path as a function of kinetic energy. The mean free path can be calculated using Equation 5, given a thin even film with a known coverage. We used the annealed CoMCTPP monolayer left on the surface after annealing to 480 K and above as a reference for a thin even film with a coverage we define to be one monolayer. Specifically, for each kinetic energy, we used the average C 1s to Ti 3p intensity ratio of all CoMCTPP measurements in the temperature range 480–500 K. Using Equation 5, we can now calculate the inelastic mean free paths of the photoelectrons in units of CoMCTPP monolayers, see Figure 4, and we get 0.39, 0.52, 0.82, and 1.17 ML for 100, 200, 400 and 700 eV, respectively. For the mean free paths in units of CoTPP monolayers see the right axis in Figure 4.

We could in principle have used the CoTPP monolayers as our reference instead. However, we found the CoMCTPP monolayers to be more reproducible, possibly because of the strong covalent bond to the surface. Furthermore, CoMCTPP monolayers are tilted[14i] and more densely packed than the flat-lying CoTPP monolayers.[16] This results in stronger attenuation and hence a better determination of the mean free paths.

The kinetic-energy dependency of Figure 3 provides a nice qualitative understanding of the three-dimensional growth of CoMCTPP and the mostly layer-by-layer growth of CoTPP.

However, to convert this kinetic-energy dependency into a more tangible unit, such as a roughness in nanometers or monolayers, a model is needed. It will never be a precise model; it will never provide the same detailed topological picture of the surface you can get from scanning probes techniques, such as AFM. Nevertheless, it will give a fair idea of the roughness required to cause the observed kinetic-energy dependency.

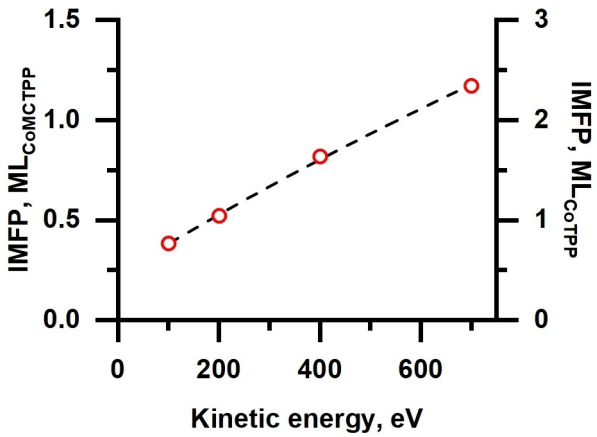

Figure 4. Inelastic mean free paths measured for CoMCTPP as a function of kinetic energy. The circles are our experimental data, while the dashed line is the best fit ($0.0058 \cdot E_{kin}/\ln(0.045 \cdot E_{kin})$) to the form of the Bethe equation suggested by Tanuma, Powell and Penn et al. for kinetic energies between 50 and 2000 eV.[27] The left axis is in units of CoMCTPP monolayers and the right in units of CoTPP monolayers (see text for details).

Keeping in mind that this is not meant to be a precise model: We chose a simple two-dimensional sine wave to describe height variations across our thin films, see Figure 5:

$$h(x,\ y) = \ h_{avg} + R \cdot \sin(x) \cdot \sin(y) \tag{6}$$

where $h(x,\ y)$ is the height at the position $(x,\ y)$, h_{avg} is the average height, and R is the height variation around the average height. The thickest point of the film now becomes $h_{avg} + R$ and the thinnest $h_{avg} - R$. Although in literature roughness is often defined as the standard deviation,[28] we will from this point on simply refer to R as the roughness of our films. Because XPS is not sensitive to the periodicity of the oscillations, x and y will remain dimensionless.

For each point in our rough surface we can now use Equations 1 and 2 to calculate the local C 1s and Ti 3p intensities. Integrating the local intensities across the whole surface gives us the global C 1s and Ti 3p intensities, which we can divide with each other to calculate the observed carbon-to-titanium intensity ratio for the surface:

$$I_C = I_C^0 \cdot \ \frac{1}{4\pi^2} \int_{x=0}^{2\pi} \int_{y=0}^{2\pi} (1 - \exp(-\ h(x,\ y)/\lambda))\ dx\ dy \tag{7}$$

$$I_{Ti} = I_{Ti}^0 \cdot \ \frac{1}{4\pi^2} \int_{x=0}^{2\pi} \int_{y=0}^{2\pi} \exp(-\ h(x,\ y)/\lambda)\ dx\ dy \tag{8}$$

$$I_{C/Ti} = I_C^0/I_{Ti}^0 \frac{\int_{x=0}^{2\pi} \int_{y=0}^{2\pi} (1 - \exp(-\ h(x,\ y)/\lambda) dx\ dy)}{\int_{x=0}^{2\pi} \int_{y=0}^{2\pi} \exp(-\ h(x,\ y)/\lambda)\ dx\ dy} \tag{9}$$

We do this for each kinetic energy, fit the ratios to our measured data from Figure 3, and then extract the roughnesses and average heights that yield the best fit to the data using the least squares method. Since the roughnesses of the films appear constant until multilayer desorption sets in, we used the average C 1s to Ti 3p intensities in the temperature range 360–440 K (9 points) to calculate the roughnesses of the CoMCTPP films and 360–390 K (4 points) for CoTPP, see Figure 3.

Figure 6 (left) shows the best fits of the measured intensities for the measurements displayed in Figure 3. The modelled $I_{C/Ti}$ intensity ratios (lines) nicely describe the experimentally measured variations in apparent thickness as a function of kinetic energy. Another way to display the same data is to compare the apparent thicknesses from Figure 3 with those predicted by the model, see Figure 6 (right). The agreement is good at low coverage, but at higher coverages the experimentally measured apparent thicknesses for 400 and 700 eV are closer together than predicted by our model. This is not surprising, as the surface is not a perfect two-dimensional sine wave. To reach a better agreement between model and measurement, a more detailed understanding of the film growth would be needed, but that is beyond the scope of this study.

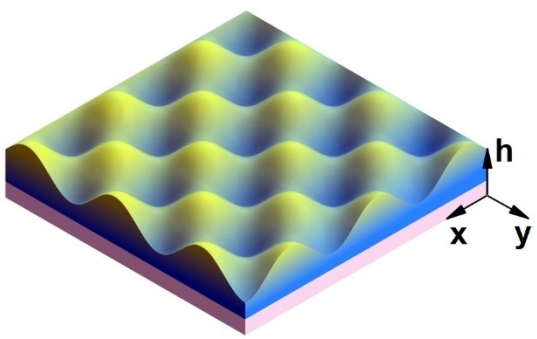

Figure 5. Schematic illustration of the two-dimensional-sine-wave model we use to describe surface roughness.

Figure 7 displays the roughnesses of the two films as a function of deposited amount (calculated as the average thickness in the model). The shaded areas indicate the thickness distribution from thinnest $(h_{avg}-R)$ to thickest $(h_{avg}+R)$ point. For CoTPP, the deposited films are smooth and even at the lowest coverage (1.1 $ML_{CoMCTPP} = 2.2\ ML_{CoTPP}$), whereas for CoMCTPP, with carboxylic anchor groups, the as-deposited films are rough from the very beginning. For both molecules, the roughness increases with increasing film thickness, and, interestingly, the increase in roughness per monolayer deposited is almost identical for both molecules. This suggests very similar multilayer growth behaviors for the two molecules, despite the presence of the carboxylic anchor group in CoMCTPP.

The roughness of CoTPP at the lowest coverage is interesting: At a coverage of 1.1 $ML_{CoMCTPP}$ corresponding to 2.2 ML_{CoTPP} the roughness of the CoTPP films is negligible. This means that the first two layers of CoTPP must wet the surface completely. The behavior of CoMCTPP at low coverages is also interesting. We do not have a measurement at exactly 1 $ML_{CoMCTPP}$, the lowest coverage of CoMCTPP we have is 1.5 $ML_{CoMCTPP}$, but extrapolating our data predicts an as-deposited one-monolayer film to have a significant roughness. This is in contrast to the annealed monolayer of CoMCTPP we use as a reference for a flat, even film, indicating that elevated temperatures are required to form a smooth CoMCTPP monolayer. A reason for this could be that elevated temperatures are required for COMCTPP molecules with carboxylic-acid anchor groups to become mobile on the surface, whereas the mostly van-der-Waals bonded CoTPP molecules are expected to have a very high mobility even at room temperature. CoMCTPP could therefore be expected to grow in a more disordered, more porous and less densely-packed structure at room temperature compared to the annealed monolayer.

4. Conclusions

We have shown how kinetic-energy-dependent XPS can be used as a fast and efficient technique for measuring thicknesses and roughnesses of thin films in one measurement. Despite the inability of XPS to provide the detailed topological information that is possible with scanning probe techniques, XPS remains a viable option when you want to characterize thin films using a single descriptor, such as roughness, over a large parameter

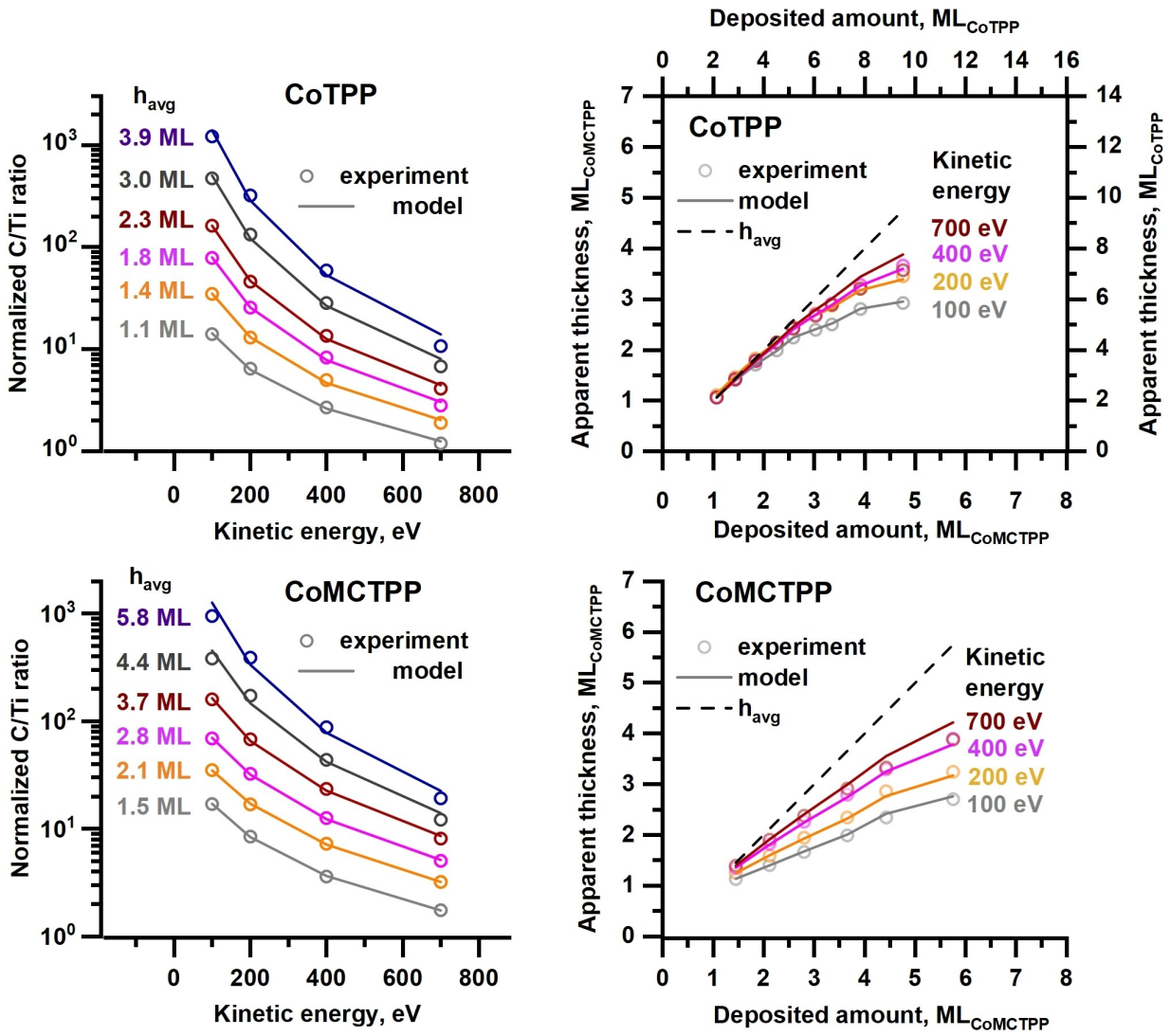

Figure 6. Left, experimentally measured (points) and modelled (lines) normalized C/Ti intensity ratios ($I_{C/Ti}/I^0_{C/Ti}$) as a function of kinetic energy and coverage for CoTPP and CoMCTPP. Right, the same data, but displayed as apparent coverages plotted as a function of the deposited amount (average thickness) yielded by the best fit to the model. The black dashed line 1:1 line represents the expected behavior for a uniform film.

space, and could even be done in situ, e.g. during heating. The method resembles other techniques, such as X-ray reflectivity,[29] where a model of the surface has to be applied to extract information from the measured data.

Specifically, we investigated the growth of CoMCTPP, with carboxylic-acid anchor groups, and CoTPP, without anchor groups, on rutile TiO_2(110). For CoTPP, the first two layers grow in a layer-by-layer fashion, but additional layers result in rougher and rougher films. This is similar to the behavior observed by Kowarik et al. for diindenoperylene on SiO_2.[5a] CoMCTPP, in contrast, exhibit three-dimensional growth at room temperature across the whole coverage range studied. Whereas thermal rearrangement was previously observed for porphyrin thin films on SiO_2,[7] we did not observe any thermal rearrangement below multilayer desorption for either of our two molecules.

We expect the roughness of the CoMCTPP films at low coverage to be caused by a low mobility of the carboxylic-acid anchor groups, creating a disordered open structure in the first as-deposited layer, which is in strong contrast to the smooth and even monolayer resulting from multilayer desorption. An interesting question is how the multilayer growth of CoMCTPP would be affected if the annealed monolayer were to be used as template, instead of the disordered as-deposited room temperature film.

We hope to have shed some new light on the growth behavior of porphyrin films that will be useful in the design of new hybrid organic /oxide materials for catalysis, organic electronics, and light-harvesting.

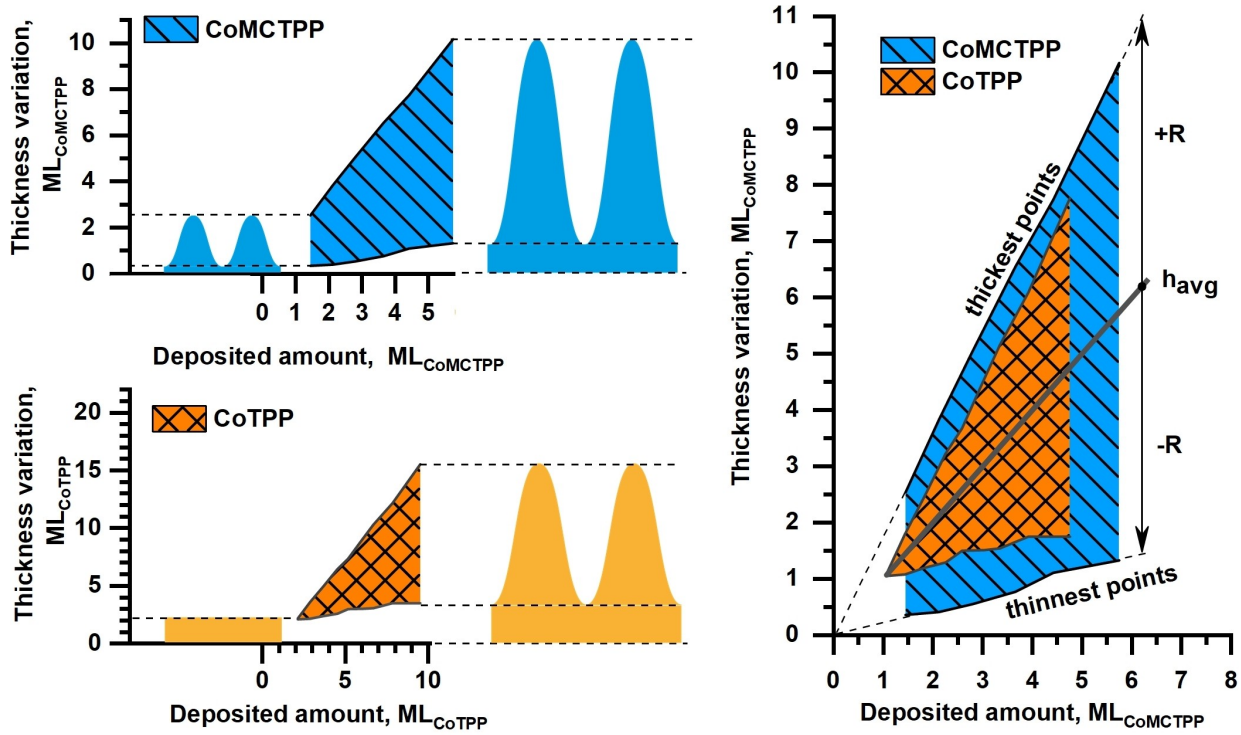

Figure 7. Distribution of thicknesses yielded by our two-dimensional-sine-wave model for CoTPP (orange) and CoMCTPP (blue) films as function of deposited amount (average thickness). To understand the figure, consider the example of 3 ML of CoMCTPP deposited on TiO_2(110). This will result in a film where the thinnest point is 0.5 ML thick, according to the two-dimensional-sine-wave model, and the thickest point 5.5 ML, meaning a roughness of 2.5 ML. Depositing the same amount of CoTPP will result in a thinnest point of 1.5 ML and a thickest point of 4.5 ML equal to a roughness of 1.5 ML. On the left two figures the thickness variations for the lowest and highest deposited amounts are also indicated by the sine-wave illustrations.

Experimental Section

The experiments were performed at the Materials Science beamline at ELETTRA Synchrotron, Trieste. Normal-emission XP spectra were acquired using a SPECS Phoibos 150 electron energy analyzer and the base pressure in the chamber was below $5 \cdot 10^{-10}$ mbar. All spectra were normalized to the photon flux, measured with a gold mesh. To be able to follow the attenuation of the photoelectron intensities across several orders of magnitude, the widest possible monochromator slits were used, producing very broad but also very intense peaks, see Figure 2.

The 5×10 mm^2 rutile TiO_2(110) single crystal (CrysTec) was cleaned by repeated cycles of Ar^+ sputtering and annealing to 700 K, producing the expected (1×1) LEED pattern. The surface cleanliness was checked with XPS and the carbon contamination was found to be below 0.06 ML. Because it is a highly-ordered single-crystal with a nice LEED pattern, the TiO_2(110) surface is expected to cause significant photoelectron diffraction, affecting the intensities of the emitted Ti 3p photoelectrons. However, as the structure of the TiO_2(110) surface is expected to remain unchanged upon adsorption and multilayer growth, the effect of photoelectron diffraction is a constant already included in I^0_{Ti}. Furthermore, because of the large size of the porphyrin and the low degree of ordering, photoelectron diffraction or back-scattering are expected to average out for the porphyrin layers, leaving the C 1s photoelectrons unaffected.

CoTPP and CoMCTPP (purchased from Porphyrin Systems Hombrecher e.K.) were evaporated using home-built Knudsen cells with graphite crucibles kept at 640–660 K. During deposition the pressure in preparation chamber would rise to $2 \cdot 10^{-8}$ mbar. The purchased batch of molecules were previously characterized by infrared spectroscopy before and after deposition.[30,31] By slowly moving a shutter in front of the TiO_2(110) sample during evaporation, gradually shadowing more and more of the sample, we created coverage gradients in the vertical direction, while keeping the coverage constant in the horizontal direction. Moving the shutter in this way means the first layer is deposited quickly across the entire sample, passivating the surface and preventing adsorption of background contaminants. The gradients allowed us to study multiple coverages on each sample. Prolonged exposure of the porphyrins films to X-rays resulted in noticeable beam damage, presumably cross-linking of molecules, observable as multilayer molecules remaining on the surface at temperatures above multilayer desorption. To reduce this effect, we moved horizontally, along the constant-coverage direction, to new measurement positions after every second annealing step.

Acknowledgements

This project was financially supported by the Deutsche Forschungsgemeinschaft (DFG) within the Research Unit FOR 1878 funCOS – Functional Molecular Structures on Complex Oxide Surfaces. F.J.W. acknowledges support from the Argentine National Council of Scientific and Technical Research (CONICET). F.J.W. thanks DFG for financial funding through a Mercator Fellowship. CERIC-ERIC consortium and Czech Ministry of Education (LM2015057) are acknowledged for the access to experimental facilities and financial support. We also are very grateful to

Kevin C. Prince for his support during the measurements and for critical reading of the manuscript. Open access funding enabled and organized by Projekt DEAL.

Conflict of Interest

The authors declare no conflict of interest.

Keywords: X-ray photoelectron spectroscopy · Growth · Porphyrin molecules · Thin films

[1] a) C. D. Dimitrakopoulos, D. J. Mascaro, *IBM J. Res. Dev.* **2001**, *45*, 11–27; b) C. D. Dimitrakopoulos, P. R. L. Malenfant, *Adv. Mater.* **2002**, *14*, 99–117; c) M. M. Ling, Z. N. Bao, *Chem. Mater.* **2004**, *16*, 4824–4840; d) H. Sirringhaus, *Adv. Mater.* **2014**, *26*, 1319–1335; e) D. Knipp, R. A. Street, A. Völkel, J. Ho, *J. Appl. Phys.* **2003**, *93*, 347–355.

[2] a) B. Kippelen, J.-L. Brédas, *Energy Environ. Sci.* **2009**, *2*, 251; b) G. Bauer, P. Würfel in: *Organic Photovoltaics: Concepts and Realization* (Eds.: C. J. Brabec, V. Dyakonov, J. Parisi, N. S. Sariciftci), Springer, Berlin Heidelberg, **2013**, 118–158; c) K. A. Mazzio, C. K. Luscombe, *Chem. Soc. Rev.* **2015**, *44*, 78–90.

[3] a) A. Dodabalapur, *Solid State Commun.* **1997**, *102*, 259–267; b) H. Sasabe, J. Kido, *J. Mater. Chem. C* **2013**, *1*, 1699; c) A. P. Kulkarni, C. J. Tonzola, A. Babel, S. A. Jenekhe, *Chem. Mater.* **2004**, *16*, 4556–4573.

[4] a) Z. Wang, H. Chang, T. Wang, H. Wang, D. Yan, *J. Phys. Chem. B* **2014**, *118*, 4212–4219; b) H. Yang, T. J. Shin, M.-M. Ling, K. Cho, C. Y. Ryu, Z. Bao, *J. Am. Chem. Soc.* **2005**, *127*, 11542–11543; c) F. Nishiyama, T. Yokoyama, T. Kamikado, S. Yokoyama, S. Mashiko, *Appl. Phys. Lett.* **2006**, *88*, 253113.

[5] a) S. Kowarik, A. Gerlach, S. Sellner, F. Schreiber, L. Cavalcanti, O. Konovalov, *Phys. Rev. Lett.* **2006**, *96*, 125504; b) D. Kafer, L. Ruppel, G. Witte, C. Woll, *Phys. Rev. Lett.* **2005**, *95*, 166602.

[6] a) A. Tersigni, J. Shi, D. T. Jiang, X. R. Qin, *Phys. Rev. B* **2006**, *74*, 205326; b) D. G. de Oteyza, E. Barrena, S. Sellner, J. O. Ossó, H. Dosch, *J. Phys. Chem. B* **2006**, *110*, 16618–16623; c) K. Werner, S. Mohr, M. Schwarz, T. Xu, M. Amende, T. Döpper, A. Görling, J. Libuda, *J. Phys. Chem. Lett.* **2016**, *7*, 555–560.

[7] a) M. M. El-Nahass, A. H. Ammar, A. A. M. Farag, A. A. Atta, E. F. M. El-Zaidia, *Solid State Sci.* **2011**, *13*, 596–600; b) H. M. Zeyada, M. M. Makhlouf, M. A. Ali, *Jpn. J. Appl. Phys.* **2016**, *55*, 022601–22608.

[8] a) J. M. Gottfried, *Surf. Sci. Rep.* **2015**, 70, 259–379; b) W. Auwarter, D. Ecija, F. Klappenberger, J. V. Barth, *Nat. Chem.* **2015**, *7*, 105–120.

[9] A. N. Oldacre, M. R. Crawley, A. E. Friedman, T. R. Cook, *Chem. Eur. J.* **2018**, *24*, 1–5.

[10] S. Ishihara, J. Labuta, W. Van Rossom, D. Ishikawa, K. Minami, J. P. Hill, K. Ariga, *Phys. Chem. Chem. Phys.* **2014**, *16*, 9713–9746.

[11] a) M. Jurow, A. E. Schuckman, J. D. Batteas, C. M. Drain, *Coord. Chem. Rev.* **2010**, *254*, 2297–2310; b) C. M. Drain, J. T. Hupp, K. S. Suslick, M. R. Wasielewski, X. Chen, *J. Porphyrins Phthalocyanines* **2002**, *06*, 243–258.

[12] C. M. Drain, A. Varotto, I. Radivojevic, *Chem. Rev.* **2009**, *109*, 1630–1658.

[13] M. Urbani, M. Gratzel, M. K. Nazeeruddin, T. Torres, *Chem. Rev.* **2014**, *114*, 12330–12396.

[14] a) M. Stark, S. Ditze, M. Drost, F. Buchner, H.-P. Steinrück, H. Marbach, *Langmuir* **2013**, *29*, 4104–4110; b) H. Marbach, *Acc. Chem. Res.* **2015**, *48*, 2649–2658; c) T. E. Shubina, H. Marbach, K. Flechtner, A. Kretschmann, N. Jux, F. Buchner, H.-P. Steinrück, T. Clark, J. M. Gottfried, *J. Am. Chem. Soc.* **2007**, *129*, 9476–9483; d) W. Hieringer, K. Flechtner, A. Kretschmann, K. Seufert, W. Auwärter, J. V. Barth, A. Görling, H.-P. Steinrück, J. M. Gottfried, *J. Am. Chem. Soc.* **2011**, *133*, 6206–6222; e) K. Diller, A. C. Papageorgiou, F. Klappenberger, F. Allegretti, J. V. Barth, W. Auwarter, *Chem. Soc. Rev.* **2016**, *45*, 1629–1656; f) P. S. Deimel, R. M. Bababrik, B. Wang, P. J. Blowey, L. A. Rochford, P. K. Thakur, T. L. Lee, M. L. Bocquet, J. V. Barth, D. P. Woodruff, D. A. Duncan, F. Allegretti, *Chem. Sci.* **2016**, *7*, 5647–5656; g) N. Ballav, C. Wäckerlin, D. Siewert, P. M. Oppeneer, T. A. Jung, *J. Phys. Chem. Lett.* **2013**, *4*, 2303–2311; h) M. Franke, F. Marchini, N. Jux, H. P. Steinruck, O. Lytken, F. J. Williams, *Chem. Eur. J.* **2016**, *22*, 8520–8524; i) D. Wechsler, C. C. Fernández, H.-P. Steinrück, O. Lytken, F. J. Williams, *J. Phys. Chem. C* **2018**, *122*, 4480–4487; j) C. C. Fernández, D. Wechsler, T. C. R. Rocha, H.-P. Steinrück, O. Lytken, F. J. Williams, *Surf. Sci.* **2019**, *689*; k) L. Zajac, P. Olszowski, S. Godlewski, L. Bodek, B. Such, R. Jöhr, R. Pawlak, A. Hinaut, T. Glatzel, E. Meyer, M. Szymonski, *Appl. Surf. Sci.* **2016**, *379*, 277–281; l) J. Schneider, M. Franke, M. Gurrath, M. Rockert, T. Berger, J. Bernardi, B. Meyer, H. P. Steinruck, O. Lytken, O. Diwald, *Chem. Eur. J.* **2016**, *22*, 1744–1749; m) M. Franke, D. Wechsler, Q. Tariq, M. Rockert, L. Zhang, P. Kumar Thakur, N. Tsud, S. Bercha, K. Prince, T. L. Lee, H. P. Steinruck, O. Lytken, *Phys. Chem. Chem. Phys.* **2017**, *19*, 11549–11553; n) M. Röckert, M. Franke, Q. Tariq, D. Lungerich, N. Jux, M. Stark, A. Kaftan, S. Ditze, H. Marbach, M. Laurin, J. Libuda, H.-P. Steinrück, O. Lytken, *J. Phys. Chem. C* **2014**, *118*, 26729–26736; o) J. Köbl, T. Wang, C. Wang, M. Drost, F. Tu, Q. Xu, H. Ju, D. Wechsler, M. Franke, H. Pan, H. Marbach, H.-P. Steinrück, J. Zhu, O. Lytken, *ChemistrySelect* **2016**, *1*, 6103–6105; p) M. Rockert, M. Franke, Q. Tariq, S. Ditze, M. Stark, P. Uffinger, D. Wechsler, U. Singh, J. Xiao, H. Marbach, H. P. Steinruck, O. Lytken, *Chem. Eur. J.* **2014**, *20*, 8948–8953; q) D. Wechsler, M. Franke, Q. Tariq, L. Zhang, T.-L. Lee, P. K. Thakur, N. Tsud, S. Bercha, K. C. Prince, H.-P. Steinrück, O. Lytken, *J. Phys. Chem. C* **2017**, *121*, 5667–5674; r) J. Schneider, F. Kollhoff, J. Bernardi, A. Kaftan, J. Libuda, T. Berger, M. Laurin, O. Diwald, *ACS Appl. Mater. Interfaces* **2015**, *7*, 22962–22969; s) J. Schneider, F. Kollhoff, T. Schindler, S. Bichlmaier, J. Bernardi, T. Unruh, J. Libuda, T. Berger, O. Diwald, *J. Phys. Chem. C* **2016**, *120*, 26879–26888.

[15] a) F. Buchner, I. Kellner, W. Hieringer, A. Gorling, H. P. Steinruck, H. Marbach, *Phys. Chem. Chem. Phys.* **2010**, *12*, 13082–13090; b) D. C. Lee, G. M. Morales, Y. Lee, L. Yu, *Chem. Commun. (Camb.)* **2006**, 100–102.

[16] G. Lovat, D. Forrer, M. Abadia, M. Dominguez, M. Casarin, C. Rogero, A. Vittadini, L. Floreano, *Phys. Chem. Chem. Phys.* **2015**, *17*, 30119–30124.

[17] a) F.-J. Meyer Zu Heringdorf, M. C. Reuter, R. M. Tromp, *Nature* **2001**, *412*, 517–520; b) G. Witte, K. Hänel, S. Söhnchen, C. Wöll, *Appl. Phys. A* **2005**, *82*, 447–455; c) S. Zorba, Y. Shapir, Y. Gao, *Phys. Rev. B* **2006**, *74*, 245104–245105; d) R. Resel, N. Koch, F. Meghdadi, G. Leising, W. Unzog, K. Reichmann, *Thin Solid Films* **1997**, *305*, 232–242; e) G. Zhang, B. L. Weeks, *Appl. Surf. Sci.* **2010**, *256*, 2363–2366.

[18] D. J. Mascaro, M. E. Thompson, H. I. Smith, V. Bulović, *Org. Electron.* **2005**, *6*, 211–220.

[19] W. Häßler-Grohne, D. Hüser, K.-P. Johnsen, C. G. Frase, H. Bosse, *Meas. Sci. Technol.* **2011**, *22*, 094003, 1–8.

[20] a) D. Kong, G. Wang, Y. Pan, S. Hu, J. Hou, H. Pan, C. T. Campbell, J. Zhu, *J. Phys. Chem. C* **2011**, *115*, 6715–6725; b) A. R. Vearey-Roberts, H. J. Steiner, S. Evans, I. Cerrillo, J. Mendez, G. Cabailh, S. O'Brien, J. W. Wells, I. T. McGovern, D. A. Evans, *Appl. Surf. Sci.* **2004**, *234*, 131–137.

[21] K. Siegbahn, *J. Electron Spectrosc. Relat. Phenom.* **1974**, *5*, 3–97.

[22] M. P. Seah, *Surface analysis by Auger and x-ray photoelectron spectroscopy* (Eds.:D. B. and J. T. Grant), IMPublications, Manchester, UK, **2003**, pp. 345–375.

[23] a) C. J. Powell, A. Jablonski, *J. Electron Spectrosc. Relat. Phenom.* **2010**, *178–179*, 331–346; b) R. C. Chatelier, H. A. W. St John, T. R. Gengenbach, P. Kingshott, H. J. Griesser, *Surf. Interface Anal.* **1997**, *25*, 741–746.

[24] a) M. Lexow, T. Talwar, B. S. J. Heller, B. May, R. G. Bhuin, F. Maier, H. P. Steinrück, *Phys. Chem. Chem. Phys.* **2018**, *20*, 12929–12938; b) A. I. Martín-Concepción, F. Yubero, J. P. Espinós, S. Tougaard, *Surf. Interface Anal.* **2004**, *36*, 788–792; c) J. Zemek, *Anal. Sci.*, **2010**, *26*, 177–186.

[25] C. S. Fadley, *J. Electron Spectrosc. Relat. Phenom.* **2010**, *178–179*, 2–32.

[26] M. Grabau, S. Krick Calderón, F. Rietzler, I. Niedermaier, N. Taccardi, P. Wasserscheid, F. Maier, H.-P. Steinrück, C. Papp, *Surf. Sci.* **2016**, *651*, 16–21.

[27] S. Tanuma, C. J. Powell, D. R. Penn, *Surf. Interface Anal.* **2011**, *43*, 689–713.

[28] E. S. Gadelmawla, M. M. Koura, T. M. A. Maksoud, I. M. Elewa, H. H. Soliman, *J. Mater. Process. Technol.* **2002**, *123*, 133–145.

[29] P. K. Palomaki, A. Krawicz, P. H. Dinolfo, *Langmuir*, **2011**, 27, 4613–4622.

[30] F. Kollhoff, J. Schneider, G. Li, S. Barkaoui, W. Shen, T. Berger, O. Diwald, J. Libuda, *Phys. Chem. Chem. Phys.* **2018**, 20, 24858–24868.

[31] T. Wahler, R. Schuster, J. Libuda, *Chem. Eur. J.* **2020**, 10.1002/chem.202001331.

Manuscript received: July 2, 2020
Revised manuscript received: August 6, 2020
Accepted manuscript online: August 21, 2020
Version of record online: September 25, 2020